PHOTOSYNTHETICA 42 (2): 193-199, 2004

Interaction of photosystem 2-LHC2 supercomplexes in adjacent layers of stacked chloroplast thylakoid membranes

L. BUMBA[*,**,+], M. HUŠÁK[***], and F. VÁCHA[**,***]

Faculty of Biological Sciences, University of South Bohemia, Branišovská 31, 370 05 České Budějovice, Czech Republic[*]
Institute of Plant Molecular Biology, Academy of Sciences of the Czech Republic, Branišovská 31, 370 05 České Budějovice, Czech Republic[**]
Institute of Physical Biology, University of South Bohemia, Branišovská 31, 370 05 České Budějovice, Czech Republic[***]

Abstract

Two types of photosystem 2-light-harvesting complex 2 (PS2-LHC2) supercomplexes with similar pigment and protein composition were isolated directly from thylakoid membranes by sucrose density gradient centrifugation. Electron microscopy and single particle image analysis revealed the first type as single unpaired PS2-LHC2 supercomplexes, whereas the second type was characterized as pairs of two PS2-LHC2 supercomplexes attached together by their stromal sides. Unstacking of thylakoid membranes resulted in a spontaneous disintegration of the paired supercomplexes into single unpaired particles. A model of the organisation of the pigment-protein complexes in grana region is proposed.

Additional key words: electron microscopy; membrane proteins; model; photosynthesis; photosystem 2; *Pisum*; single particle image analysis.

Introduction

Primary reactions of oxygenic photosynthesis occur in thylakoid membranes of chloroplasts, algae, and cyanobacteria. They are catalyzed by several pigment-protein complexes: photosystem 2 (PS2), photosystem 1 (PS1), their light-harvesting antenna complexes, and a complex of cytochrome (cyt) b_6/f. In chloroplasts of higher plants and green algae, thylakoid membranes are differentiated into stacked (grana) and unstacked (stroma lamellae) membrane regions. The membrane stacking is mediated by the presence of Mg^{2+} cations (Izawa and Good 1966, Murata 1969) and results in formation of grana regions containing mainly PS2 and its light-harvesting antenna complexes (Andersson and Anderson 1980, Barber 1980, Chow *et al*. 1991, Vácha *et al.* 2000, Mustardy and Garab 2003).

Photon energy is predominantly harvested by major and minor light-harvesting complex (LHC2) consisting of several integral chlorophyll *a*/*b*-binding proteins (Green and Durnford 1996). The major LHC2 complexes form trimers containing mixture of Lhcb1-3 proteins in different ratios. The structure of LHC2 was solved at a resolution of 0.34 nm by electron crystallography (Kühlbrandt *et al.* 1994). The minor antennae proteins CP29, CP26, and CP24 (Lhcb4-6) are in a monomeric form and regulate the excitation energy transfer to the reaction centre of PS2. The whole PS2 complex contains more than 25 subunits. Some of them are involved in photochemical reactions resulting in a reduction of plastoquinone and oxidation of water to molecular oxygen (Barber *et al.* 1997, Hankamer *et al.* 2001a). Recently, structure of the PS2 core complex from two cyanobacteria strains has been solved at a resolution of 0.37–0.38 nm by X-ray (Zouni *et al.* 2001, Kamiya and Shen 2003) and from spinach at a resolution of 0.9 nm by electron crystallography (Hankamer *et al.* 2001b).

PS2 complex forms, together with its light-harvesting antenna complexes, the so-called PS2-LHC2 supercomplex (for reviews see Hankamer *et al.* 1997a, Bumba and Vácha 2003). Electron microscopy (EM) with single particle image analysis have revealed that a central part of the supercomplex is formed by a dimeric PS2 core complex surrounded by two symmetry-related structures, each

Received 8 January 2004, *accepted* 26 February 2004.
[+]Corresponding author; fax: +420-38-5310356, e-mail: bumba@umbr.cas.cz
Abbreviations: Chl – chlorophyll; CP – chlorophyll protein; cyt – cytochrome; DCBQ – 2,5-dichloro-*p*-benzoquinone; DM – *n*-dodecyl-*β*-D-maltoside; EM – electron microscopy; LHC2 – light-harvesting complex; OEC – oxygen evolving complex; PS – photosystem; SDS-PAGE – sodium dodecyl sulphate-polyacrylamide gel electrophoresis.
Acknowledgements: This work was supported, in part, by the grants of the Ministry of Education, Youth, and Sports of the Czech Republic FRVS 1292/2002 (L.B.), CEZ 12300001 (M.H.), LN00A141, and GACR 206/03/1107 (F.V.).

consisting of one trimeric LHC2 and monomeric CP29 and CP26 proteins (Boekema *et al.* 1995, Hankamer *et al.* 1997b, Harrer *et al.* 1998). In addition, a three-dimensional model of the supercomplex has revealed the location of proteins of oxygen-evolving complex (Nield *et al.* 2000). This supercomplex may also bind CP24 protein and one or more additional LHC2 trimers at various positions (Boekema *et al.* 1998b, 1999, Yakushevska *et al.* 2001).

Although it has been suggested that the PS2-LHC2 supercomplex forms the basic unit of PS2 in a large part of the thylakoid membranes, principle of the interaction of supercomplexes in adjacent membranes within the grana is not well understood yet. We present the electron microscopy and single particle image analysis of two types of PS2-LHC2 supercomplexes isolated directly from stacked and unstacked thylakoid membranes.

Materials and methods

Stacked thylakoid membranes were prepared from fresh, dark-adapted, 21-d-old pea plants grown in a greenhouse condition. The pea leaves were suspended in an ice cold buffer A (50 mM Hepes, pH 7.6, 0.4 M sorbitol, 5 mM $MgCl_2$, 2 mM EDTA, 2 mM ascorbate) and homogenized by five short (5 s) pulses in a blender. The homogenate was filtered through 12 layers of cotton wool and the filtrate was centrifuged for 4 min at 3 000×*g*. The pellet was homogenized in a buffer B (50 mM Hepes, pH 7.6, 0.4 M sorbitol, 5 mM $MgCl_2$) and centrifuged at 3 000×*g* for 10 min. The resulting pellet was washed in a buffer C (50 mM Hepes, pH 7.6, 5 mM $MgCl_2$) and incubated in dark on ice for 15 min. The suspension was then centrifuged for 10 min at 20 000×*g* and re-suspended in a buffer D (50 mM Hepes, pH 7.6, 0.4 M sorbitol, 5 mM $MgCl_2$, 20 % glycerol, v/v). Unstacked thylakoid membranes were prepared as above, but $MgCl_2$ was omitted from all buffers.

Continuous sucrose density gradient was prepared by freezing and thawing. The centrifuge tubes were filled with 20 mM Mes, pH 6.5, 10 mM NaCl, 5 mM $CaCl_2$, 0.03 % *n*-dodecyl-*β*-D-maltoside (DM), and 0.6 M sucrose, and frozen at –20 °C. Slow thawing at 4 °C resulted in a formation of the continuous sucrose density gradient (0–1.2 M). Thylakoid membranes (1 mg Chl per cm^3) were solubilized by 20 mM DM and 200 mm^3 of the homogenate was loaded onto a freshly prepared sucrose density gradient. Centrifugation was carried out at 4 °C using a *P56ST* rotor (*Hitachi*) at 550 rps for 13.5 h.

Protein composition was determined by SDS-PAGE using a 12–20 % linear gradient polyacrylamide gel containing 6 M urea in the buffer system of Laemmli (1970). For immunoblotting, proteins were separated by SDS-PAGE and transferred to a nitrocellulose membrane (0.1 μm, *Schleicher&Schuell*, Germany) followed by incubation with primary antibodies raised against synthetic peptides of light-harvesting chlorophyll *a/b*-binding (Lhcb) proteins (*Agrisera*, Sweden). Immunoblots were visualized by a colorimetric reaction with anti-rabbit IgG secondary antibody (*Sigma*) conjugated with alkaline phosphatase.

Oxygen evolution was measured using a Clark-type oxygen electrode (*Hansatech*). Samples at a chlorophyll concentration of 10 μg per cm^3 were suspended to a medium containing 20 mM Mes (pH 6.5), 0.3 M sucrose, 20 mM $CaCl_2$, 10 mM $NaHCO_3$, 10 mM NaCl, and 500 μM 2,5-dichloro-*p*-benzoquinone (DCBQ) and irradiated with "white light". Room temperature absorption spectra were measured using a *Spectronic Unicam UV300* (*Spectronic*, UK). Fluorescent emission spectra were measured using a *Fluorolog* spectrofluorometer (*Spex*, USA) at 77 K with excitation wavelength 430 nm (excitation to Chl *a*).

For electron microscopy, freshly prepared supercomplexes were subjected to *Sephadex 200* column to remove sucrose from the sample. The specimen was placed on glow-discharged carbon-coated copper grids and negatively stained with 2 % uranyl acetate. Electron microscopy was performed with a *Philips TEM 420* electron microscope (*Philips*) using 80 kV at 60 000× magnification. Micrographs were digitized with a pixel size corresponding to 0.51 nm at the specimen level. Image analyses were carried out using *SPIDER* software package (Frank *et al.* 1996). From 37 micrographs of the band *E* and from 25 micrographs of the band *F*, about 6 200 and 3 500 particle projections were selected for analysis, respectively. The selected projections were rotationally and translationally aligned, and treated by multivariate statistical analysis in combination with classification (van Heel and Frank 1981, Harauz *et al.* 1988). Classes from each of the subsets were used for refinement of alignments and subsequent classifications. For the final sum, the best of the class members were summed, using a cross-correlation coefficient of the alignment procedure as a quality parameter.

Results

Sucrose density gradient centrifugation of stacked thylakoid membranes solubilized with mild detergent β-dodecyl-maltoside (DM) resulted in a separation of six green bands (*A*-*F*, Fig. 1, *left*). All bands were characterized by their protein composition and absorption and 77 K fluorescence emission spectra. These results indicated that bands *A, B, C,* and *D* were enriched in monomeric LHC2, trimeric LHC2, monomeric PS2 core complex,

and the PS1-LHC1 supercomplex, respectively (Fig. 2*A*). The two lowest green bands (*E* and *F*) showed similar characteristics in pigment and protein composition. Based on SDS-PAGE analysis, both bands contained the major subunits of PS2 (CP47, CP43, D2, D1, α- and β-subunits of cyt b_{559}, and 33, 23, and 16 kDa extrinsic proteins (Fig. 2*A*, lanes *E* and *F*). The immunoblot analysis of the Lhcb proteins associated with PS2 in bands *E* and *F* showed the presence of major LHC2 (Lhcb1 and Lhcb2), CP29 (Lhcb4), CP26 (Lhcb5), and very small amounts of CP24

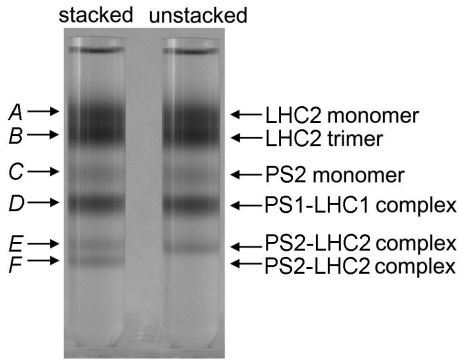

Fig. 1. Sucrose density gradient ultracentrifugation of stacked (*left*) and unstacked (*right*) pea thylakoid membranes. Stacked and unstacked thylakoid membranes were solubilized with *n*-dodecyl-*β*-D-maltoside and separated in a linear 0 to 1.2 M sucrose gradient. The composition of each chlorophyll-containing band is indicated on the right.

(data not shown). The band *E*, in addition to the PS2 and Lhcb proteins, was contaminated by a small amount of PS1 and LHC1 proteins. In Fig. 2*A* (lane *E*), the band around 60 kDa corresponds to the PsaA/PsaB reaction centre proteins of PS1 and several bands between 20-24 kDa to the proteins of the LHC1 complex (Scheller *et al.* 2001). Compared to the lane *E*, the lane *F* showed a higher amount of protein with a molecular mass of about 28 kDa. The immunoblots against the Lhcb proteins together with densitogram analyses revealed an increase of the Lhcb1 and Lhcb2 proteins in the lane *F* of about 21 % as compared to 28-kDa protein band in the lane *E* (data not shown). Absorption and 77 K fluorescence emission spectra of the bands *E* and *F* are presented in Figs. 2*B* and *C*, respectively. Comparison of the absorption spectra shows that the band *E* has a slightly higher absorption in the region between 460–520 nm indicating a higher carotenoid content due to the presence of residual PS1 centres. Compared with the band *F*, the band *E* shows in the 77 K fluorescence emission spectrum an additional small peak at 735 nm corresponding to emission of long-wavelength PS1 antenna LHC1-730 (see Schmid *et al*. 2002). Oxygen evolution measurements yielded 162±13 and 182±14 mmol(O_2) kg^{-1}(Chl) s^{-1} for the bands *E* and *F*, respectively. These results are in a good agreement with previous studies of a PS2-LHC2 supercomplex indicating that both bands *E* and *F* of sucrose density gradient contain the PS2-LHC2 supercomplex (Boekema *et al.* 1995).

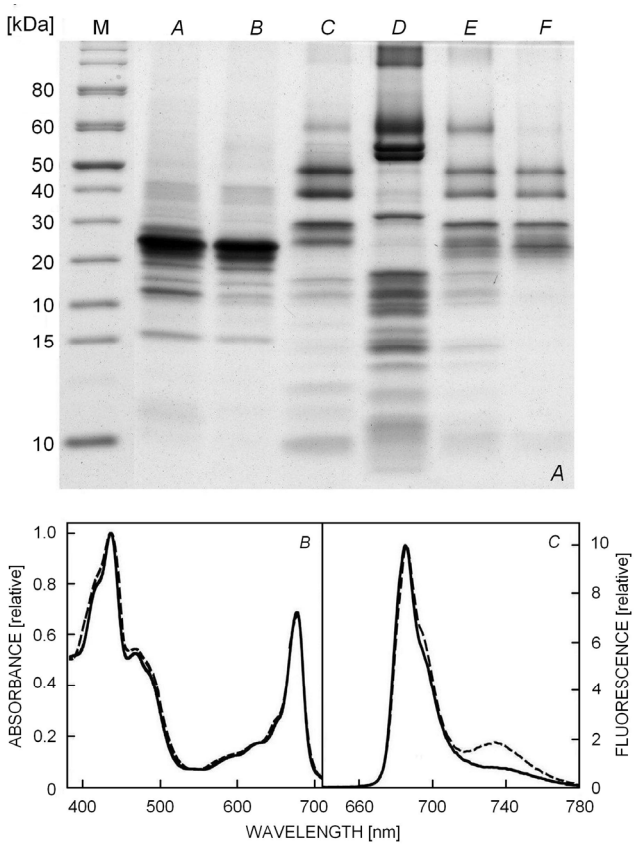

Fig. 2. *A*: SDS-PAGE analysis of six green bands from the sucrose density gradient. Lane M, markers of molecular masses [kDa] are indicated on the left. Lane *A*, monomeric Lhcb polypeptides; lane *B*, major trimeric LHC2 complex; lane *C*, monomeric PS2 core complex; lane *D*, PS1-LHC1 complex; lanes *E* and *F*, PS2-LHC2 supercomplexes. *B*: Room temperature absorption spectra of PS2-LHC2 supercomplexes from bands *E* (*dashed line*) and *F* (*solid line*). *C*: 77 K fluorescence emission spectra of PS2-LHC2 supercomplexes from bands *E* (*dashed line*) and *F* (*solid line*). The spectra were normalized at 438 (absorption) and 685 (fluorescence) nm, respectively.

Electron microscopy of negatively stained PS2-LHC2 supercomplexes revealed marked differences between the *E* and *F* green bands. EM images of the band *E* revealed predominantly rectangular-shaped particles of the PS2-LHC2 supercomplex in their top-view projection (Fig. 3*A*). A total of 5 300 projections were aligned, treated with multivariate statistical analysis, and classified into 6 classes (Fig. 4). The classification showed that the supercomplex, which has been structurally described by Boekema *et al*. (1995), comprised 75 % of the data set. The projections of the supercomplex have little variation in the overall shape of the particle and differ in distribution of negative stain (Fig. 4*A–D*). In 18 % of the data set a fragment of this supercomplex, lacking one set of the Lhcb components (a mass in the upper part of the

complex in Fig. 4*E*), was present. The rest of the projection (7 %) contained oval-shaped particles (Fig. 4*F*), which are similar in size and shape to the PS1-LHC1 complex characterized by Boekema *et al.* (2000).

The classification of 2 300 particles from the EM images of the band *F* revealed only side-view projection of two PS2-LHC2 supercomplexes aggregated by their stromal sides into pairs (Fig. 5*A–C*). No other type of particles was present (Fig. 3*B*). A single protrusion located at the centre of the lumen surface of the supercomplex and less visible additional densities on each side of this central protrusion correspond to the extrinsic 33 and 23 kDa proteins (Fig. 5*A,B*), respectively (Boekema *et al.* 1998a). From the data set of paired supercomplex, about 6 % of projection was shorter in length indicating different binding of the paired supercomplex to the support carbon film (Fig. 5*C*).

In order to determine physiological relevance of paired supercomplexes *in vivo*, thylakoid membranes were isolated in the absence of Mg^{2+} ions. Separation of DM-solubilized unstacked membranes by sucrose density gradient centrifugation resulted in five green bands (*A–E*, Fig. 1, *right*). As compared to the stacked thylakoid membranes, no green band corresponding to the band *F* of stacked membranes was presented. The band *E* (E^{-Mg}) of the unstacked membranes was associated with approximately twice higher chlorophyll content compared with the band *E* of stacked membranes. Protein composition and spectral properties of the E^{-Mg} band were almost identical to its stacked counterpart and the EM with image analysis did not reveal any significant changes in the E^{-Mg} band particle projections compared with the particles of the band *E* of stacked membranes (data not shown).

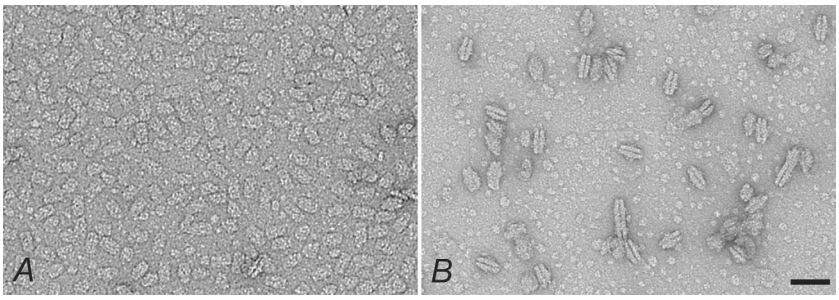

Fig. 3. Electron micrographs of PS2-LHC2 supercomplexes obtained from sucrose density gradient band *E* **(***A***)** and band *F* (*B*), negatively stained with 2 % uranyl acetate. *The scale bar* represents 50 nm.

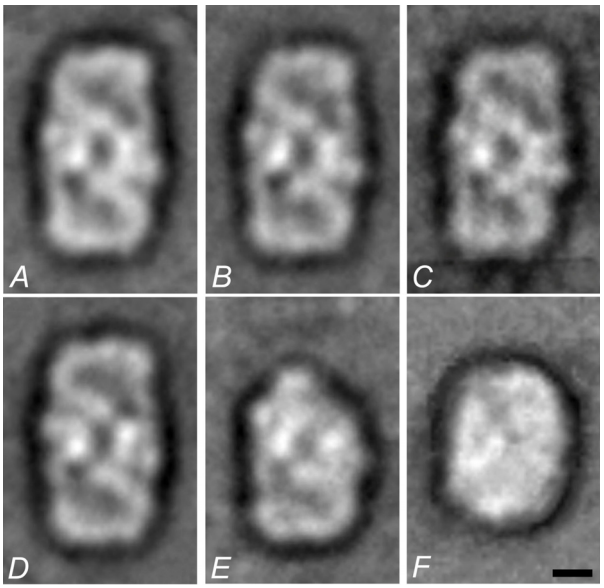

Fig. 4. Results of multivariate statistical analysis and classification of top-view projections of PS2-LHC2 supercomplexes obtained from sucrose density gradient band *E*. Results were obtained from the classification of a set of 5 300 supercomplex projections, which were decomposed into 6 classes. Average projections represent single unpaired PS2-LHC2 supercomplex (*A-D*), the fragment of the PS2-LHC2 supercomplex lacking one set of Lhcb components (*E*), and monomeric PSI-LHCI complexes (*F*). The number of summed images is: 430 (*A*), 375 (*B*), 117 (*C*), 495 (*D*), 345 (*E*), and 85 (*F*). *The scale bar* represents 5 nm.

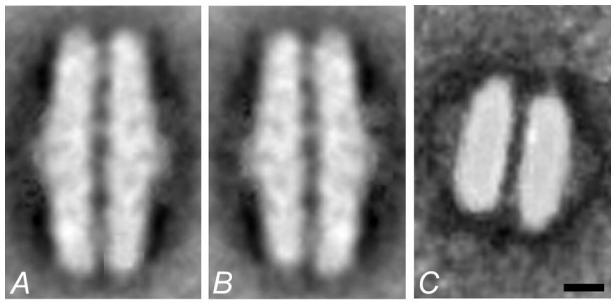

Fig. 5. Results of multivariate statistical analysis and classification of side-view projections of PS2-LHC2 supercomplexes obtained from sucrose density gradient band *F*. Results were obtained from the classification of a set of 2 300 supercomplex projections, which were decomposed into 3 classes. Average projections represent paired PS2-LHC2 supercomplex composed of two single unpaired supercomplexes attached with their stromal surfaces. The number of summed images is: 285 (*A*), 315 (*B*), 58 (*C*). *The scale bar* represents 5 nm.

Discussion

PS2-LHC2 supercomplex has been previously isolated using sucrose density gradient centrifugation (Hankamer *et al.* 1997b, Eshaghi *et al.* 1999) or gel filtration chromatography (Boekema *et al.* 1998b, 1999). However, we were able to distinguish two populations of the PS2-LHC2 supercomplex isolated from stacked thylakoid membranes using sucrose density gradient centrifugation. In our case, two bands of the PS2-LHC2 supercomplex with similar pigment and protein composition were resolved in sucrose density gradient centrifugation in contrast to only one supercomplex band reported previously (Eshaghi *et al.* 1999). The structural features of projections of both types of PS2-LHC2 supercomplexes are highly similar with those previously reported (Boekema *et al.* 1995, 1998a, Nield *et al.* 2000), but now, paired and unpaired supercomplexes are separated into two distinct green bands on the sucrose density gradient.

The band F contains only proteins of the PS2-LHC2 supercomplex and should be considered as the pure PS2-LHC2 supercomplex (Hankamer *et al.* 1997b). Small differences in pigment and protein composition between the bands *E* and *F* are thus produced, in part, by the contamination of the band *E* with the PS1-LHC1 supercomplex and by a heterogeneity in the protein composition of the PS2-LHC2 supercomplex itself. The presence of the PS1-LHC1 supercomplex in the band *E* is indicated on the SDS-PAGE (Fig. 2*A*) by 77 K fluorescence emission spectrum (Fig. 2*C*) as well as by the presence of the oval particle obtained after the single particle analysis steps (Fig. 4*F*) that correspond to the PS1-LHC1 supercomplex (Boekema *et al.* 2001). A small heterogeneity observed in the unpaired PS2-LHC2 supercomplex corresponds to the presence of the fragment of this supercomplex (Fig. 4*E*). Such fragment has been previously described and suggested to be a supercomplex lacking one set of the Lhcb components (Boekema *et al.* 1998b). A comparison of amounts of the Lhcb subunits in the bands *E* and *F* shows an increase of the Lhcb1 and Lhcb2 proteins in the lane *F* of about 21 % as compared to the lane *E*. The decrease of 21 % in the amount of the Lhcb subunits in the band *E* corresponded to the finding that 18 % of the particle data set contains the fragment of the supercomplex lacking one set of Lhcb subunits.

Despite the differences, our results indicated that top-view projections of the band *E* correspond to the unpaired PS2-LHC2 particles (*i.e.* single supercomplexes), whereas side-view projections of the band *F* correspond to the paired PS2-LHC2 supercomplexes (aggregates of two single supercomplexes from adjacent membranes). The unpaired supercomplexes were more susceptible to detergent treatment as shown by the appearance of their fragments in contrast to the paired population, which seems to be more stable due to interactions between the neighbouring particles. Since we used the concentration of Mg^{2+} ions close to that observed in intact chloroplasts, the presence of both, paired and unpaired, populations of the supercomplexes in the gradient led to the suggestion that paired supercomplexes exist *in vivo* in thylakoid membrane.

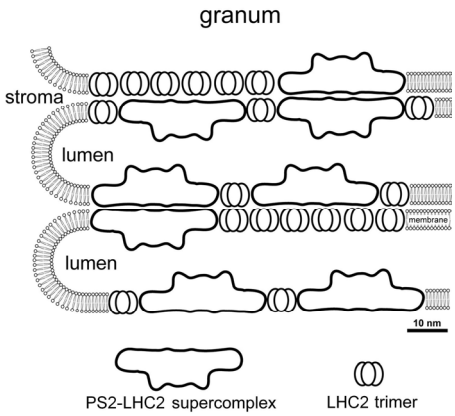

Fig. 6. A schematic representation of the organisation of photosynthetic pigment-protein complexes in grana region of the thylakoid membrane of higher plants. One part of PS2-LHC2 supercomplexes is organized into paired populations in two adjacent grana membranes. The rest of PS2-LHC2 supercomplexes is attached to free LHC2 trimers of the adjacent grana thylakoid membrane.

To approve this assumption, unstacked thylakoid membranes were isolated in the absence of Mg^{2+} ions, solubilized by DM, and subjected to sucrose density gradient centrifugation (Fig. 1*A*). The disappearance of the band *F* in company with increment of the intensity of band *E* in the gradient suggests that in the absence of Mg^{2+} ions the paired supercomplexes are disintegrated into single unpaired counterparts found consecutively in the band *E*. The loss of the band *F* also supports the evidence that artificial aggregation of the particles into the paired supercomplexes in the gradient was avoided. It was found previously that the formation of paired supercomplexes is observed in case of using EM grids without previous 'activation' of the carbon support film by a glow-discharge apparatus (unpublished result). Due to the strong hydrophobicity of the carbon film before 'activation', particles tend to aggregate changing their native appearance. In our case, all preparation was done with glow-discharged carbon films and thus artificial formation of paired supercomplexes was avoided.

Our results suggest that a part of the PS2-LHC2 supercomplexes is present in the two adjacent grana membranes in paired populations (Fig. 6). The paired PS2-LHC2 supercomplexes were previously observed in adjacent layers of stacked grana membranes (Boekema *et al.* 2000). Since the presence of bivalent cations is most important in the formation of stacked membranes (Jennings and Forti 1974, Barber and Mills 1976, Gross *et al.* 1976, Murata 1969, Allen and Forsberg 2001), their

elimination lead to the complete randomization of the grana parts (Staehelin 1976, Telfer *et al.* 1976) and consequently to disappearing of paired supercomplexes. The presence of unpaired population of the PS2-LHC2 supercomplexes in stacked membranes can be explained either by partial dissociation of the paired complexes during solubilization or by the fact that part of these supercomplexes do not have their counterpart supercomplexes in the other layer. As it is demonstrated in Fig. 6 we suppose, together with conclusions of Boekema *et al*. (2000), that many PS2-LHC2 supercomplexes in one membrane layer face only LHC2 in the counterpart layer. However, the PS2-LHC2 supercomplexes attached with LHC2 complexes in adjacent membrane were not observed in our preparations. This would imply a complete solubilization of the counterpart LHC2 complexes from the PS2-LHC2 supercomplexes indicating lower binding forces between the PS2-LHC2 supercomplexes and LHC2 which is probably necessary to enable a free lateral distribution of LHC2 among PS2 complexes for optimal distribution of excitation energy.

References

Allen, J.F., Forsberg, J.: Molecular recognition in thylakoid structure and function. – Trends Plant Sci. **6**: 317-326, 2001.

Andersson, B., Anderson, J.M.: Lateral heterogeneity in the distribution of chlorophyll-protein complexes of the thylakoid membranes of spinach chloroplasts. – Biochim. biophys. Acta **593**: 427-440, 1980.

Barber, J.: Membrane surface charges and potentials in relation to photosynthesis. – Biochim. biophys. Acta **594:** 253-308, 1980.

Barber, J., Mills, J.: Control of chlorophyll fluorescence by the diffuse double layer. – FEBS Lett. **68**: 288-292, 1976.

Barber, J., Nield, J., Morris, E.P., Zheleva, D., Hankamer, B.: The structure, function and dynamics of photosystem two. – Physiol. Plant. **100**: 817-827, 1997.

Boekema, E.J., Hankamer, B., Bald, D., Kruip, J., Nield, J., Boonstra, A.F., Barber, J., Rögner, M.: Supramolecular structure of the photosystem II complex from green plants and cyanobacteria. – Proc. nat. Acad. Sci. USA **92**: 175-179, 1995.

Boekema, E.J., Jensen, P.E., Schlodder, E., van Breemen, J.F.L., van Roon, H., Scheller, V.H., Dekker, J.P.: Green plant photosystem I binds light-harvesting complex I on one side of the complex. – Biochemistry **40**: 1029-1036, 2001.

Boekema, E.J., Nield, J., Hankamer, B., Barber, J.: Localization of the 23-kDa subunit of the oxygen evolving complex of photosystem II by electron-microscopy. – Eur. J. Biochem. **252**: 268-276, 1998a.

Boekema, E.J., van Breemen, J.F.L., van Roon, H., Dekker, J.P.: Arrangement of photosystem II supercomplexes in crystalline macrodomains within the thylakoid membrane of green plant chloroplasts. – J. mol. Biol. **301**: 1123-1133, 2000.

Boekema, E.J., van Roon, H., Calkoen, F., Bassi, R., Dekker, J.P.: Multiple types of association of photosystem II and its light-harvesting antenna in partially solubilized photosystem II membranes. – Biochemistry **38**: 2233-2239, 1999.

Boekema, E.J., van Roon, H., Dekker, J.P.: Specific association of photosystem II and light-harvesting complex II in partially solubilized photosystem II membranes. – FEBS Lett. **424**: 95-99, 1998b.

Bumba, L., Vácha, F.: Electron microscopy in structural studies of Photosystem II. – Photosynth. Res. **77**: 1-19, 2003.

Chow, W.S., Miller, C., Anderson, J.M.: Surface charges, the heterogenous lateral distribution of the two photosystems, and thylakoid stacking. – Biochim. biophys. Acta **1057**: 69-77, 1991.

Eshaghi, S., Andersson, B., Barber, J.: Isolation of a highly active PS2-LHC2 supercomplex from thylakoid membranes by a direct method. – FEBS Lett. **446**: 23-26, 1999.

Frank, J., Radermacher, M., Penczek, P., Zhu, J., Li, Y.H., Ladjadj, M., Leith, A.: SPIDER and WEB: Processing and visualization of images in 3D electron microscopy and related fields. – J. struct. Biol. **116**: 190-199, 1996.

Green, B.R., Durnford, D.G.: The chlorophyll-carotenoid proteins of oxygenic photosynthesis. – Annu. Rev. Plant Physiol. Plant mol. Biol. **47**: 685-714, 1996.

Gross, E.L., Zimmermann, R.J., Hormats, G.F.: The effect of mono- and divalent cations on the quantum yields for electron transport in chloroplasts. – Biochim. biophys. Acta **440**: 59-67, 1976.

Hankamer, B., Barber, J., Boekema, E.J.: Structure and membrane organization of photosystem II in green plants. – Annu. Rev. Plant Physiol. Plant mol. Biol. **48**: 641-671, 1997a.

Hankamer, B., Morris, E.P., Nield, J., Carne, A., Barber, J.: Subunit positioning and transmembrane helix organisation in the core dimer of photosystem II. – FEBS Lett. **504**: 142-151, 2001a.

Hankamer, B., Morris, E., Nield, J., Gerle, C., Barber, J.: Three-dimensional structure of the photosystem II core dimer of higher plants determined by electron microscopy. – J. struct. Biol. **135**: 262-269, 2001b.

Hankamer, B., Nield, J., Zheleva, D., Boekema, E., Jansson, S., Barber, J.: Isolation and biochemical characterization of monomeric and dimeric photosystem II complexes from spinach and their relevance to the organization of photosystem II in vivo. – Eur. J. Biochem. **243**: 422-429, 1997b.

Harauz, G., Boekema, E., van Heel, M.: Statistical image analysis of electron micrographs of ribosomal subunits. – Methods Enzymol. **164**: 35-49, 1988.

Harrer, R., Bassi, R., Testi, M.G., Schafer, C.: Nearest-neighbor analysis of a photosystem II complex from *Marchantia polymorpha* L. (liverwort), which contains reaction center and antenna proteins. – Eur. J. Biochem. **255**: 196-205, 1998.

Izawa, S., Good, N.E.: Effect of salts and electron transport on the conformation of isolated chloroplasts. II. Electron microscopy. – Plant Physiol. **41**: 544–552, 1966.

Jennings, R.C., Forti, G.: The influence of magnesium on the chlorophyll fluorescence yield of isolated chloroplasts. – Biochim. biophys. Acta **347**: 299-310, 1974.

Kamiya, N., Shen, J.R.: Crystal structure of oxygen-evolving photosystem II from *Thermosynechococcus vulcanus* at 3.7-angstrom resolution. – Proc. nat. Acad. Sci. USA **100**: 98-103, 2003.

Kühlbrandt, W., Wang, D.N., Fujiyoshi, Y.: Atomic model of plant light-harvesting complex by electron crystallography. –

Nature **367**: 614-621, 1994.

Laemmli, U.K.: Cleavage of structural proteins during the assembly of the head of bacteriophage T4. – Nature **227**: 680-685, 1970.

Murata, N.: Control of excitation transfer in photosynthesis. II. Magnesium ion-dependent distribution of excitation energy between two pigment systems in spinach chloroplasts. – Biochim. biophys. Acta **189**: 171-181, 1969.

Mustardy, L., Garab, G.: Granum revisited. A three-dimensional model – where things fall into place. – Trends Plant Sci. **8**: 117-122, 2003.

Nield, J., Orlova, E.V., Morris, E.P., Gowen, B., van Heel, M., Barber, J.: 3D map of the plant photosystem II supercomplex obtained by cryoelectron microscopy and single particle analysis. – Nature struct. Biol. **7**: 44-47, 2000.

Scheller, H.V., Jensen, P.E., Haldrup, A., Lunde, C., Knoetzel, J.: Role of subunits in eukaryotic Photosystem I. – Biochim. biophys. Acta **1507**: 41-60, 2001.

Schmid, V.H.R., Potthast, S., Wiener, M., Bergauer, V., Paulsen, H., Storf, S.: Pigment binding of photosystem I light-harvesting proteins. – J. biol. Chem **277**: 37307-37314, 2002.

Staehelin, L.A.: Reversible particle movements associated with unstacking and restacking of chloroplast membranes *in vitro*. – J. Cell Biol. **71**: 136-158, 1976.

Telfer, A., Nicolson, J., Barber, J.: Cation control of chloroplast structure and chlorophyll *a* fluorescence yield and its relevance to the intact chloroplast. – FEBS Lett. **65**: 77-83, 1976.

Vácha, F., Vácha, M., Bumba, L., Hashizume, K, Tani, T.: Inner structure of intact chloroplasts observed by a low temperature laser scanning microscope. – Photosynthetica **38**: 493-496, 2000.

van Heel, M., Frank, J.: Use of multivariate statistics in analyzing the images of biological macromolecules. – Ultramicroscopy **6**: 187-194, 1981.

Yakushevska, A.E., Jensen, P.E., Keegstra, W., van Roon, H., Scheller, H.V., Boekema, E.J., Dekker, J.P.: Supermolecular organization of photosystem II and its associated light-harvesting antenna in *Arabidopsis thaliana*. – Eur. J. Biochem. **268**: 6020-6028, 2001.

Zouni, A., Witt, H.T., Kern, J., Fromme, P., Krauss, N., Saenger, W., Orth, P.: Crystal structure of photosystem II from *Synechococcus elongatus* at 3.8 Å resolution. – Nature **409**: 739-743, 2001.